High-Pressure Intrinsic Oxidation Kinetics of Two Coal Chars

ARTICLE *in* ENERGY & FUELS · FEBRUARY 2003

Impact Factor: 2.79 · DOI: 10.1021/ef020195r

6 AUTHORS, INCLUDING:

William C. Hecker
Brigham Young University - Provo Main Cam…
103 PUBLICATIONS **1,010** CITATIONS
SEE PROFILE

Thomas H. Fletcher
Brigham Young University - Provo Main Cam…
155 PUBLICATIONS **2,299** CITATIONS
SEE PROFILE

High-Pressure Intrinsic Oxidation Kinetics of Two Coal Chars

William C. Hecker, Peter M. Madsen, Michael R. Sherman, Jared W. Allen, Rebecca J. Sawaya, and Thomas H. Fletcher*

Chemical Engineering Department, 350 CB, Brigham Young University, Provo, Utah 84602

Received September 4, 2002

Chars were produced from two coals (North Dakota lignite and Pittsburgh No. 8 hva bituminous coal) in a flat flame burner at atmospheric pressure. Intrinsic char reactivities to oxygen were then measured in a high-pressure thermogravimetric analyzer as a function of temperature, total pressure, and partial pressure of oxygen. Care was taken to avoid mass transfer effects. Reactivities were normalized by the available mass of char at any given time ($g/(g_{avail}\cdot s)$). Reactivity data were obtained over a wide range of char burnout and were found to be independent of burnout level between char burnouts of 20 and 60%. Data were obtained at pressures from 1 to 32 atm and at temperatures from 598 to 823 K and were analyzed using the *n*th order rate law and Arrhenius temperature dependence. The reaction order of each char was shown to be constant at 0.7 for total pressures ranging from 1 to 32 atm and for partial pressures of oxygen ranging from 0.03 to 12.8 atm, and was essentially the same for both chars. Activation energies determined for each char were also determined to be constant with total pressure and partial pressure of O_2.

Introduction

Char oxidation at elevated pressures is important in a number of energy conversion applications, including high-pressure coal gasification and pressurized fluidized bed reactors. High-pressure coal applications have the potential to decrease the cost of producing electricity and to allow for greater control of emissions from coal-fired power plants. In particular, high-pressure gasifiers that are often oxygen blown and combined with a gas turbine cycle are being considered to increase efficiency of electric power generation and therefore reduce CO_2 evolution. Furthermore, pressurized flue gas streams may facilitate the removal of pollutants.

The kinetics of char oxidation at atmospheric pressure have been studied extensively; however, kinetic data for char oxidation at elevated pressures are very limited. Suuberg and co-workers[1] reviewed the low-temperature kinetic data on the reaction of O_2 with many different chars and carbons. They also measured reaction orders and activation energies for both a phenol−formaldehyde resin char and a lignite char. The literature review indicated a variety of reported reaction orders, all between 0 and 1. Suuberg's experimental data indicated a constant order of 0.68 over a wide range of partial pressures of oxygen.

Standard kinetic models that explain char oxidation rates at atmospheric pressure often seem to fail at high pressures.[2] Two types of simple kinetic models have been proposed for high-pressure char oxidation. One is an *n*th order rate expression of the form $r = kP_{O_2}^n$, where $k = A\exp(-E_a/RT)$. The other type is a changing order expression, such as the Langmuir model of the form $r = kP_{O_2}/(1 + KP_{O_2})$. Some high-pressure studies indicate that the *n*th order model fails at high pressures; however, the available data are sparse, and conflicting conclusions have been drawn about the true form of the high-pressure rate expression.[3,4] Moreover, many existing high-pressure studies were performed under conditions where the char reaction rate was partially or fully mass transfer limited.[5] The resulting data are therefore not suitable to be used in determining fundamental kinetic models. Thus, there is a clear need for char oxidation kinetic data at high pressures.

The overall purpose of this study is to assemble a complete set of intrinsic kinetic data for char oxidation over a wide range of char types, total pressures, and oxygen partial pressures, and to use these data in the determination of a simple intrinsic rate expression for char oxidation at both low and high pressures. This paper reports intrinsic kinetic data for the oxidation of chars made at atmospheric pressure from North Dakota lignite (NDL) and from Pittsburgh No. 8 hva bituminous coal. The effects of pressure on reaction rate, reaction order, and activation energy are shown. This paper summarizes data presented in several conference proceedings.[6,7]

Experimental Section

Sample Preparation. The North Dakota lignite and the Pittsburgh No. 8 coal samples were first sieved to obtain the

* Author to whom correspondence should be addressed. Phone: (801) 422-6236. E-mail: tom_fletcher@byu.edu.

(1) Suuberg, E. M.; Wojtowicz, M.; Calo, J. M. *Proc. Combust. Inst.* **1988**, *22*, 79−87.

(2) Monson, C. R.; Germane, G. J.; Blackum, A. U.; Smoot, L. D. *Combust. Flame* **1995**, *100*, 669−683.

(3) Hong, J.; Hecker, W. C.; Fletcher, T. H. *Proc. Combust. Inst.* **2000**, *28*, 2215−2223.

(4) Essenhigh, R. H.; Mescher, A. M. *Proc. Combust. Inst.* **1996**, *26*, 3085−3094.

(5) Roberts, D. G.; Harris, D. J. *Energy Fuels* **2000**, *14* (3), 483−489.

10.1021/ef020195r CCC: $25.00
Published on Web 02/20/2003

64 to 76 μm diameter size fraction. The coal particles were injected through the center feed tube of a natural gas/air flat-flame burner at atmospheric pressure. Particles experienced a heating rate of 10^4 to 10^5 K/s, a gas temperature of 1600–1700 K, and a residence time of about 50 ms. The post-flame oxygen concentration remained at about 3 mole %, and post-flame particle velocities of 2.5 m/s were measured. These conditions were sufficient to complete the devolatilization process with only small amounts of char oxidation. The measured mass loss was 65% (daf) for the NDL char and 56% (daf) for the Pitt 8 char. The measured C/H ratios on a mass basis were 77 for the NDL char and 100 for the Pitt 8 char. Additional details of the char preparation are available.[6–8]

Experimental Apparatus and Conditions. Reactivity experiments were performed in a DMT (Deutsche Montan Technologie—Essen, Germany) high-pressure thermogravimetric analyzer (HPTGA) which measures sample mass continuously with time. The HPTGA consists of a reaction chamber equipped with a pressure control system, an electric heater, a highly sensitive balance, and a gas metering system, and allows for accurate control of total pressure, gas concentrations, and gas temperature. Care was taken to ensure that the experiments were carried out under conditions such that the reaction rate was controlled only by chemical processes and was not affected by mass or heat transfer effects. Temperature ranges and gas flow rates were chosen accordingly.

Experiments on the NDL char were performed under conditions ranging from 1 to 32 atm, 3 to 80% O_2, and 598 to 723 K. Slightly higher temperatures (673 to 823 K) were used for the less reactive Pitt 8 char in order to obtain data in reasonable amounts of time. After the reaction chamber of the HPTGA was brought to steady-state at the desired conditions, the wire mesh basket containing the char sample was rapidly lowered into the chamber. Sample sizes of 2 to 4 mg were used in these experiments to minimize mass transfer effects. Pressure, temperature, and mass were monitored continuously, and 1000 data points per run were recorded.

Kinetic Data Determination. Intrinsic reaction rates were determined for each experimental run. Since the HPTGA microbalance measures sample mass continuously with time, the reaction rate can be determined at any given time. The reaction rate was calculated for each of the 1000 data points (mass vs time) recorded per run. Reaction rate values were determined on a "gram reacted per gram available" basis by dividing the slope of the mass loss curve by the instantaneous mass. Three runs were performed at each experimental condition; the average reaction rate and standard deviation were then determined for each condition. The HPTGA data were reduced assuming an nth order intrinsic model. Activation energies were determined from standard Arrhenius plots ($\ln[k]$ vs $1/T$, or $\ln[\text{rate}]$ vs $1/T$ at constant oxygen concentration). Oxygen reaction orders were determined from a power law model by determining slopes of $\ln[\text{rate}]$ vs $\ln[P_{O_2}]$. Confidence intervals for the reported oxygen orders and activation energies were determined using the standard deviations of the individual sets of conditions combined with Monte Carlo simulations. The Monte Carlo simulations were performed using the Microsoft Excel normal distribution number generator to calculate 1000 points within the bounds of the standard deviations of the measured rate at each condition. Since orders and activation energies were generated from five average rates, this resulted in 1000 sets of five points. Orders and activation energies were then generated for each set of points, and the mean and standard deviation were determined. The 95% confidence interval was taken as ±2 standard deviations.

(6) Sawaya, R. J.; Allen, J. W.; Hecker, W. C.; Fletcher, T. H. *Prepr. Pap.—Am. Chem. Soc., Div. Fuel Chem.* **1999**, *44* (4), 1013–1019.

(7) Madsen, P. M.; Fletcher, T. H.; Hecker, W. C. *Prepr. Pap.—Am. Chem. Soc., Div. Fuel Chem.* **2001**, *46* (1), 318–320.

(8) Cope, R. F. Effects of Calcium Oxide and Burnout Level on Oxidation of Beulah Zap Chars. PhD. Dissertation. Brigham Young University, Provo, Utah, 1995.

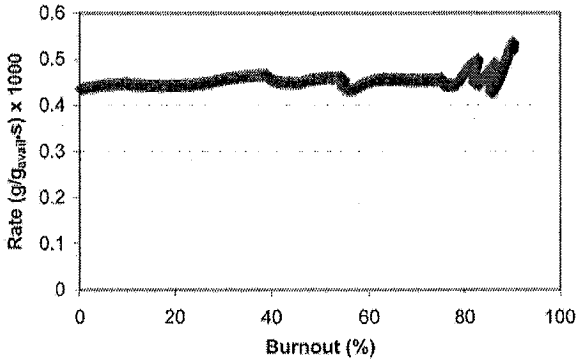

Figure 1. Reaction rate versus burnout level for a representative NDL char experiment at a temperature of 648 K, a total pressure of 8 atm, and an oxygen partial pressure of 0.8 atm.

Effect of Burnout Level on Char Oxidation Rate. Reaction rates computed on a "gram reacted per gram available" basis were found to be independent of burnout level between 20 and 60% char burnout, as shown in Figure 1 for one condition. In general, small fluctuations were observed in the char reaction rate when the char burnout was less than 10 to 15% burnout. The fluctuations in the initial rates were probably due to buoyancy effects, small amounts of volatiles, or adsorbed species. At high levels of burnout (usually greater than 70%), the measured reaction rate often began to fluctuate greatly and became unpredictable. This could have been caused by particle fragmentation or by the normalization procedure where the rate is divided by the small amount of mass remaining. In this analysis, a single value for the reaction rate of each experimental run was found by averaging the instantaneous rates that were measured at char burnouts between 20 and 60%. The range of 20 to 60% was chosen in order to be conservative.

Effect of Gas Flow Rate on Reaction Rate. The intrinsic rate of any heterogeneous reaction should depend only upon the surface reaction rate and should not be affected by heat or mass transfer effects. To reduce the chance that the observed reaction rates in this study would be affected by heat transfer effects, oxygen was used as the reaction gas in a background of helium. Since helium has higher thermal conductivity than other potential inert gases (N_2 for example), the use of helium reduces the probability that significant thermal gradients could occur. Nevertheless, early in this study, it was found that the observed reaction rate was a function of the flow rate of the reaction gas (oxygen in helium). Figure 2 shows the observed reaction rates from experiments performed at four different gas flow rates, holding all other reactor conditions constant (a temperature of 648 K, a total pressure of 8 atm, and a partial pressure of O_2 of 0.8 atm). It can be seen in Figure 2 that the observed reaction rate at the lowest flow rate (2 standard liters per minute, or slpm) was significantly lower than the observed reaction rate at the higher flow rates. However, as the flow rate increases, the observed reaction rate becomes less dependent upon flow rate and appears to become independent of gas flow rate at flow rates greater than about 5 slpm. This is evidenced by the fact that the observed reaction rates for flow rates of 6 and 8 slpm are essentially the same.

Flow rates can affect observed reaction rates by causing the mass transfer of the reacting gas to the surface to become limiting. At low gas flow rates, the time required for oxygen to diffuse through the boundary layer to the surface appears to be somewhat limiting. However, at higher flow rates, the mass transfer coefficient increases, film diffusion is no longer a limiting process, and the observed reaction rate approaches the intrinsic reaction rate. Experiments were performed at each pressure to determine the flow rate at which mass

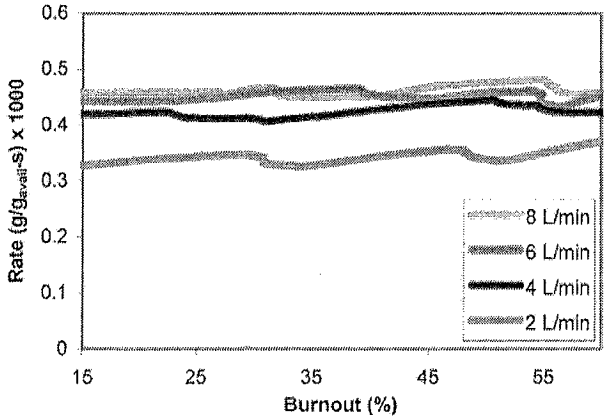

Figure 2. The effect of gas flow rate on reaction rate of NDL char for experiments performed at 648 K, 8 atm of total pressure, 0.8 atm of O_2 pressure, and at gas flow rates of 2, 4, 6, and 8 L/min.

Table 1. Experimental Conditions Used in the Determination of the Effect of Total Pressure on NDL Char Reaction Rate (temperature = 648 K)

total pressure (atm)	flow rate (slpm)	mole % O_2	oxygen partial pressure (atm)
1	4	80	0.8
4	4	20	0.8
8	6	10	0.8
16	8	5	0.8
32	10	2.5	0.8

transfer effects were not controlling. The flow rates used for the determination of char oxidation rates in this study are shown in Table 1. As shown in this table, the minimum gas flow rate required for the observed reaction rate to be independent of gas flow rate was found to increase with increasing total pressure.

Results and Discussion

Effect of Total Pressure on Reaction Rate. The effect of total pressure on intrinsic reaction rate of NDL char with O_2 was studied over a pressure range of 1 to 32 atm. Table 1 shows the experimental conditions used for the NDL char reactivity experiments at each pressure. Temperature and oxygen partial pressure were held constant in order to isolate the effects of total pressure. Figure 3 is a plot of the average reaction rate versus burnout for each of the five total pressures studied. As can be seen, reaction rate is independent of burnout (between 15 and 60%) at each of the total pressures studied. Furthermore, it can be seen that reaction rate is not a strong function of total pressure, if at all. A plot of average reaction rate (in the 20 to 60% burnout range) versus total pressure shows little pressure dependence, as shown in Figure 4. The error bars in Figure 4 represent the 95% confidence intervals, which are about $\pm 3 \times 10^{-5}$ (g/(g$_{avail}$·s)) at each pressure. It appears from Figure 4 that there is a slight trend of decreasing reaction rate with increasing total pressure. However, the observed decrease in reaction rate is quite small for a very large change in total pressure (a factor of 32). Thus, within experimental error, the intrinsic reaction rate appears to be independent of total pressure for this condition.

Effect of Total Pressure on Oxygen Order. The oxygen order of the NDL char oxidation reaction was

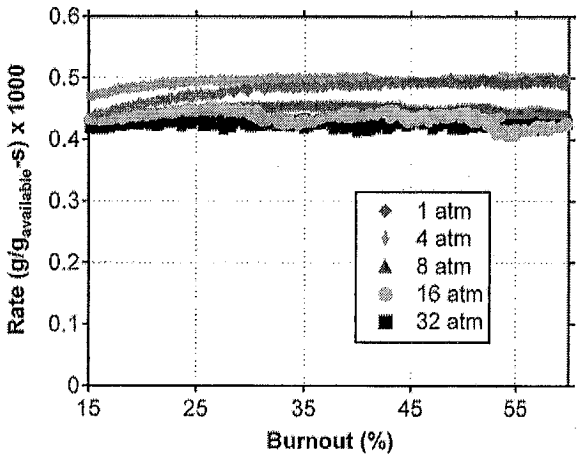

Figure 3. The effect of char burnout level on the rate of NDL char oxidation at total pressures of 1 to 32 atm. All runs were made at 648 K and at an oxygen partial pressure of 0.8 atm.

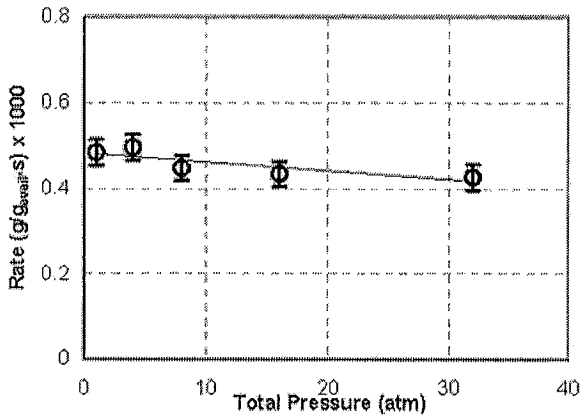

Figure 4. The effect of total pressure on average char oxidation rate for the NDL char. All experiments were performed at 648 K and 0.8 atm of oxygen partial pressure.

Table 2. Reaction Orders for NDL Char Oxidation

pressure (atm)	temperature (K)	mole fraction O_2	partial pressures of O_2	oxygen reaction order
1	648	0.03–0.80	0.03–0.80	0.70 ± 0.05
4	648	0.03–0.40	0.12–1.60	0.71 ± 0.06
8	648	0.03–0.40	0.24–3.20	0.74 ± 0.04
16	648	0.03–0.40	0.48–6.40	0.75 ± 0.02

determined at four different total pressures over a range of 1 to 16 atm, as shown in Table 2. Power law kinetics were assumed and the temperature was held constant at 648 K. Oxygen concentrations of 3, 6, 10, 20, and 40% were used at each total pressure, and an additional oxygen concentration point of 80% was used for the order determination at 1 atm total pressure. Figure 5 shows the data used to determine the reaction order at 8 atm. Each point represents an average of 2 to 4 experimental runs. The order is the slope of the line through the data points when plotting ln[rate] vs ln-$[P_{O_2}]$.

The oxygen orders of NDL char oxidation for total pressures of 1, 4, 8, and 16 atm are shown in Table 2, along with the 95% confidence intervals computed from the Monte Carlo technique. The oxygen orders and confidence intervals of the Pitt 8 char were determined

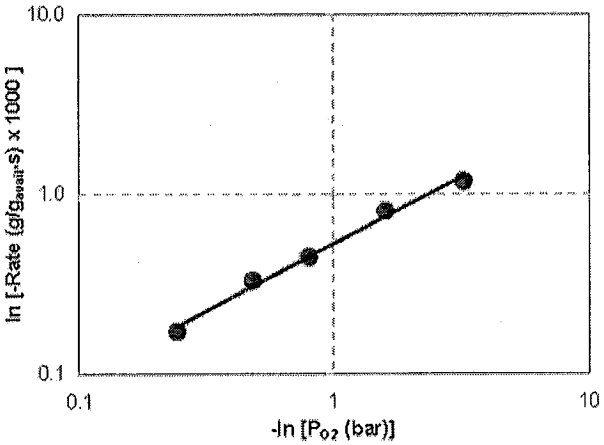

Figure 5. The effect of oxygen partial pressure on NDL char reaction rate at a total pressure of 8 atm and a temperature of 648 K. The slope is the oxygen order.

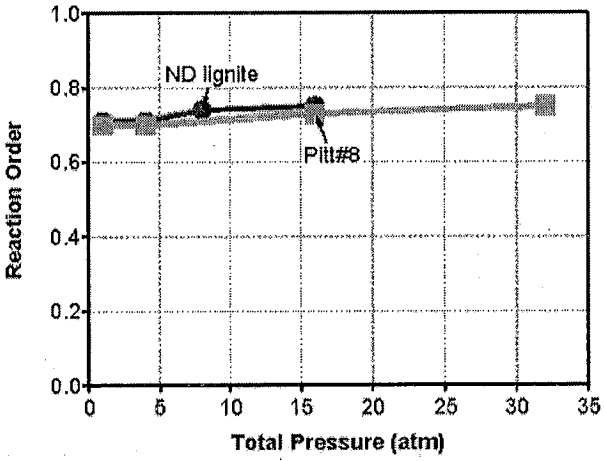

Figure 6. The effect of total pressure on the order of the NDL and Pitt 8 char reactions with oxygen.

Table 3. Reaction Orders for Pitt 8 Char Oxidation

pressure (atm)	temperature (K)	mole fraction O_2	partial pressures of O_2	oxygen reaction order
1	823	0.025–0.40	0.025–0.40	0.70 ± 0.07
4	773	0.025–0.40	0.10–1.60	0.70 ± 0.08
16	748	0.025–0.40	0.40–6.40	0.73 ± 0.08
32	723	0.025–0.40	0.80–12.80	0.75 ± 0.05

at pressures of 1, 4, 16, and 32 atm in a similar manner, as shown in Table 3. The confidence intervals for the Pitt 8 data are larger than for the NDL data; the reason for this is not clear. The reaction order data for the two chars are compared in Figure 6. The NDL data shown in Figure 6 were obtained at a temperature of 648 K, while the Pitt 8 data were obtained at temperatures ranging from 723 to 823 K. It is quite interesting that the reaction orders determined for the two chars are identical.

No strong effect of total pressure on oxygen order is seen in Figure 6. Although oxygen order does appear to increase slightly with increasing total pressure, the change in oxygen order is very small and appears to be within experimental error. It can be concluded that oxygen order is not significantly affected by changes in total pressure. This conclusion is supported by the

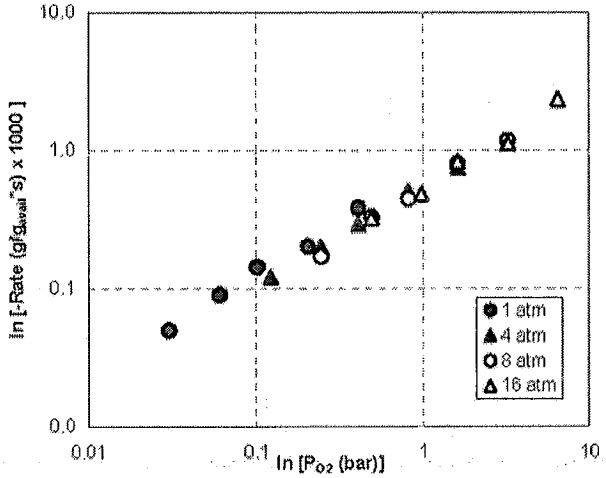

Figure 7. The effect of P_{O_2} on char oxidation rate from 0.03 to 6.4 atm P_{O_2} at 648 K for NDL char. These data were also used to determine the oxygen order at each of the four total pressures.

observed effect of oxygen partial pressure on rate over a large range of partial pressures. The data from the oxygen order determinations for the NDL char were plotted together for all of the four total pressures used. This plot is shown in Figure 7, showing the effect of oxygen partial pressure on reaction rate over a large partial pressure range (0.03 to 6.4 atm) and for four different total pressures.

Figure 7 shows that the data over the whole partial pressure range studied (a factor of about 200) are remarkably linear. The oxygen order obtained from the slope of all the data together is 0.68 ± 0.03. This overall oxygen order is essentially the same as that observed at each of the individual total pressures, suggesting that the oxygen order does not change significantly in the total pressure range of 1 to 16 atm. This order of 0.68 is precisely what was obtained for the two chars studied by Suuberg and co-workers.[1] These results show that a power law fits intrinsic char oxidation reactivities over a wide range of partial pressures of O_2, and imply that models with changing order (such as Langmuir or Langmuir–Hinshelwood models) are not appropriate in this range of conditions.

Effect of Total Pressure on Activation Energy. The effect of total pressure on activation energy was also studied over the total pressure range of 1 to 32 atm. The activation energy of the NDL char was determined at 1, 4, 8, and 16 atm by using standard Arrhenius plots. The corresponding Pitt 8 experiments were conducted at pressures of 1, 4, 16, and 32 atm. The oxygen partial pressure was held constant at 0.8 atm for the NDL char activation energy experiments, varying the mole fraction of O_2 and using a temperature range of 598 to 713 (see Table 4). The mole fraction of oxygen was held constant at 0.27 in the Pitt 8 char activation energy experiments, varying the partial pressure of O_2 and using temperatures ranging from 673 to 823 K (see Table 5). A representative Arrhenius plot used to determine the activation energy for NDL char at 8 atm is shown in Figure 8. The Arrhenius plot in Figure 8 uses the rate rather than the rate constant because the partial pressure of O_2 was held constant in the NDL experi-

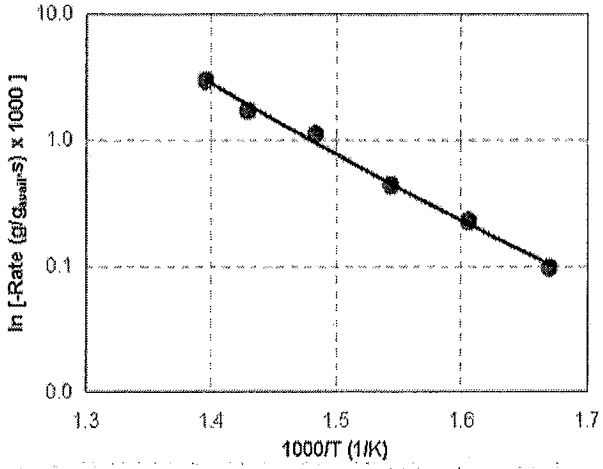

Figure 8. Arrhenius plot of NDL char reactivity data taken at 8 atm total pressure. Oxygen partial pressure is 0.8 atm and temperature ranges from 598 to 713 K.

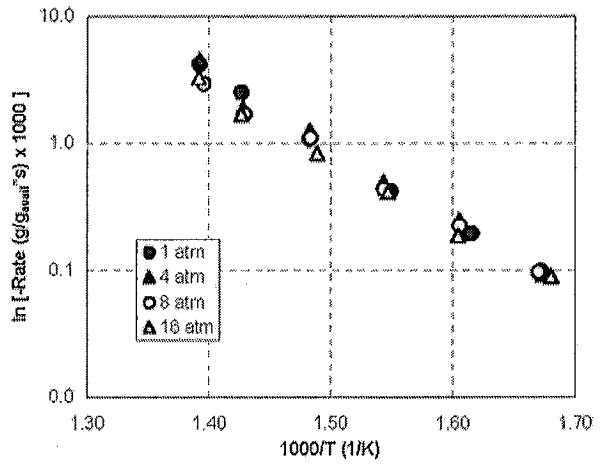

Figure 9. Arrhenius plot of NDL char oxidation rates at 1, 4, 8, and 16 atm for temperatures from 598 to 713 K. All data were obtained at 0.8 atm of oxygen partial pressure.

Table 4. Activation Energies for NDL Char Oxidation (partial pressure of O_2 = 0.8)

pressure (atm)	mole fraction O_2	temperature range (K)	activation energy (kcal/mol)
1	0.8	598–713	26.5 ± 1.2
4	0.2	598–713	26.0 ± 1.4
8	0.1	598–713	24.3 ± 1.4
16	0.05	598–713	24.5 ± 1.4

Table 5. Activation Energies for Pitt 8 Char Oxidation (mole fraction of O_2 = 0.27)

pressure (atm)	partial pressure O_2 (atm)	temperature range (K)	activation energy (kcal/mol)
1	0.27	773–823	32.7 ± 4.1
4	1.08	738–823	33.2 ± 3.1
16	4.32	723–773	33.0 ± 4.2
32	8.64	673–723	33.2 ± 5.0

ments. Since the partial pressure of O_2 was not constant in the Pitt 8 experiments, rate constants were used in the Arrhenius plots to determine activation energies.

The activation energies of NDL char and the Pitt 8 char at other pressures were determined in a similar manner, and are listed in Tables 4 and 5, respectively.

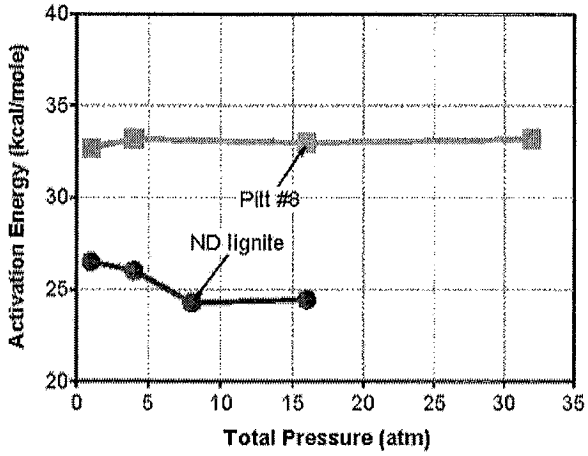

Figure 10. Effect of total pressure on activation energy of the NDL and Pitt 8 char reactivity. NDL char experiments were performed with an O_2 pressure of 0.8 atm and a temperature range of 598 to 713 K. Pitt 8 char experiments were performed with an oxygen mole fraction of 0.27 over a temperature range of 673 to 823 K.

Confidence intervals are also listed in these tables; 95% confidence intervals for the Pitt 8 char are larger than for the NDL char. When the Arrhenius plots for each of the different total pressures are compared in the same graph (see Figure 9), it can be seen that their slopes are very similar. This suggests that activation energy is not a strong function of total pressure.

A summary of the activation energy data for the NDL and Pitt 8 chars is shown in Figure 10. It appears that there may be a slight decrease in activation energy with increasing total pressure for the NDL char. This decrease is just barely above the confidence intervals determined for the activation energy (see Table 4). The activation energies for the Pitt 8 char are higher than the NDL char (as expected), but appear to be constant with pressure.

Conclusions

This study has examined the intrinsic oxidation of two coal chars prepared at high temperature and high heating rate at atmospheric pressure. High-pressure TGA experiments were conducted over a pressure range of 1 to 32 atm, a temperature range of 598 to 823 K, a range of oxygen partial pressures from 0.03 to 12.8 atm, and a burnout range of 20 to 60%. Under these conditions, it has been found that intrinsic char oxidation rate, determined on a (g/(g$_{avail}$·s)) basis, is independent of char burnout level, and that kinetic parameters are not affected by changes in total pressure. More specifically, under the conditions of this study, intrinsic char oxidation rate, activation energy, and oxygen reaction order were found to be independent of total pressure. It has also been found that the nth order kinetic model fits both atmospheric and elevated pressure char oxidation data very well, with $n = 0.7$ for both chars studied.

More work should be performed in order to firmly establish the kinetics of high-pressure char oxidation. One particular area that should be studied is the intrinsic kinetics of chars produced at elevated pressure. Since the char used in this study was produced at atmospheric pressure, it is possible that chars produced

at elevated pressures may exhibit different behavior. In addition, it is possible that the internal surface area in the char changes significantly during these experiments. Many mechanistic models of intrinsic reactivity normalize the reactivity by the internal surface area. Changes in the internal surface area may account for the changes in reactivity with total pressure or burnout predicted by some of these models. Finally, char reactivity data are needed at high temperatures as well as at high pressures.

EF020195R